ISBN: 978-981-18-5852-9
WCSE 2022 Spring Event: 2022 9th International Conference on Industrial Engineering and Applications
doi: 10.18178/wcse.2022.04.127

Decoupling Vibration Control for a Two-Link Manipulator

Qiang Xin [1 2], Chongchong Wang [2], Chin-Yin Chen [2 +], Guilin Yang [2] and Fazhan Li [3]

[1] University of Chinese Academy of Sciences, Beijing 100049, China;

[2] Zhejiang Key Laboratory of Robotics and Intelligent Manufacturing Equipment Technology, Ningbo Institute of Materials Technology and Engineering, Chinese Academy of Sciences, Ningbo 315201, China;

[3] Ningbo City College of Vocational Technology, Ningbo 315201, China

Abstract. Due to the influence of the coupling torque in the two-link manipulator, the disturbance observer (DOB) method cannot achieve an ideal vibration suppression effect. A velocity controller is proposed, including a decoupler and a rigid-body state observer (RBSO), to simultaneously decrease the coupling torque and vibrations. The two-link manipulator is modelled as a two-input two-output (TITO) system in this paper. The decoupler is designed based on the dynamic model of the TITO system in a simplified structure. The RBSO contains a state observer (SOB) and a damper. The SOB obtains a rigid-body velocity from its state variable. The damper feeds back the error between the rigid-body velocity and link velocity to a proportional-integral controller to add system damping, achieving vibration suppression. The effectiveness to decrease coupling torque and vibrations of the proposed method are verified in simulations.

Keywords: TITO system, decoupler, rigid-body state observer, coupling torque, vibrations

1. Introduction

The two-link manipulator, as the simplest type in collaborative robots, is usually modelled as a two-input two-output (TITO) system. Importantly, it needs a lightweight design to ensure the safety of human-robot interaction [1]. However, the lightweight design reduces the mechanical body's stiffness, leading to vibrations easily, which seriously affects the accuracy of motion control and the system's stability. Hence, vibration suppression research has been very urgent in recent years [2].

The vibration suppression algorithms can mainly be classified into feedforward and feedback methods. The feedforward methods, such as the input shaping method [3] and model-based feedforward method [4], do not limit by the measurement accuracy of encoders but are affected by model uncertainties. The feedback methods are more commonly used in the vibration suppression of the TITO system. The fuzzy PID method can adaptively adjust the PID parameters online by using the fuzzy logic to depress vibrations [5]. Nevertheless, the fuzzy logic requires expert knowledge [6]. The acceleration feedback method is effective to suppress vibration. While the acceleration solution error is large, or installs accelerometer needing extra cost [7]. The disturbance observer (DOB) method is more popular to suppress vibrations due to its robustness to external disturbances and model uncertainties [8, 9]. Although the DOB method has high requirements on the accuracy of its nominal model, it can observe some signals without any extra sensors, such as the acceleration or coupling torque [10].

Nevertheless, the coupling torque between adjacent joints in a TITO system is much large, which cannot be considered an external disturbance for the DOB method. Furthermore, the coupling torque significantly worse the vibration suppression effects. Therefore, aiming to achieve an ideal vibration suppression effect, the coupling torque of a TITO system also needs to be decoupled.

The decoupling algorithms for a TITO system mainly can be divided into two categories: static decoupling and dynamic decoupling [11]. The static decoupling needs less system information, which reduces the influence of model uncertainties. However, the static decoupling is designed based on steady gains. It is easy to introduce unfavorable factors in the high-frequency stage, affecting the decoupling effect [12]. The dynamic decoupling can achieve better performance but needs a more accurate system model. It includes ideal decoupling, simplified decoupling and inverted decoupling. Among these three kinds of

+ Corresponding author. Tel.: +86-0574-8760-2663.
E-mail address: chenchinyin@nimte.ac.cn.

dynamic decoupling, the simplified decoupling only needs two decoupler matrix and is easily implemented in practice [13]. In addition, there are other intelligent decoupling methods, such as adaptive control [14], neural network control [15], and so on. These intelligent methods are not strictly depending on the system model, which is easy to achieve good decoupling results. Nevertheless, they are relatively complex and time-consuming.

This paper proposes a method that combines a dynamic decoupler in a simplified structure and a rigid-body state observer (RBSO). The decoupler aims to decouple the coupling torque between adjacent joints. The RBSO aims to depress vibrations of the TITO system in a decentralized structure, which contains a state observer (SOB) and a Damper. The SOB aims to observe a rigid-body velocity, which is designed to be more robust to external disturbances and model uncertainties than traditional methods that are theoretically proven in our previous work [16]. The Damper feeds back the error between the observed rigid-body velocity and link velocity to a proportional-integral controller, adding system damping to achieve vibration suppression. The ability to decrease coupling torque and vibrations of the proposed method is verified by comparing it with a pure PI method in simulations.

2. Coupling Model of a TITO System

Fig. 1(a) shows that a two-link manipulator can be described as a TITO system. The TITO system's coupling model is established in the Laplace domain, as shown in fig. 1 (b).

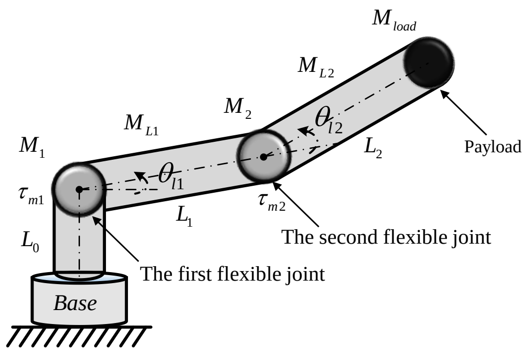

(a)

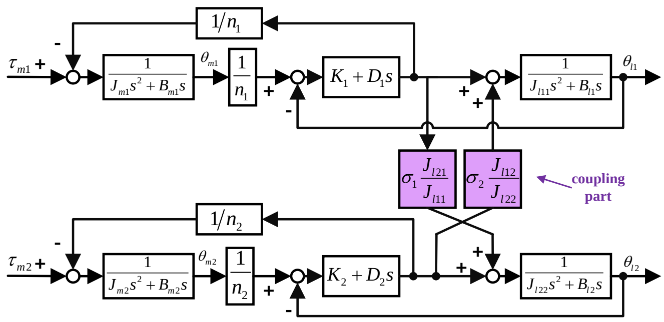

(b)

Fig. 1. (a) Diagram of a two-link manipulator. (b) The coupling model.

In fig. 1, the L_j is the length of the j^th link (j is 0, 1 or 2). M_i represents the mass of the i^th joint (i is 1 or 2). M_{Li} and M_{load} are the mass of the i^th link and the payload installed on the end of this two-link manipulator. τ_{mi} is the driving torque of the i^th joint. J_{mi}, J_{lii}, θ_{mi}, θ_{li}, B_{mi}, B_{li} and n_i are the motor-side inertia, link-side inertia, motor position, link position, motor-side viscous damping, link-side viscous damping and reduction ratio of the i^th joint, respectively. The drive chain (includes torque sensor and harmonic drive) is modelled as a linear spring K_i and damping D_i. In the coupling part, σ_1 and σ_2 are the deviation factors to simulate the unmodeled dynamic coupling errors.

The link-side inertia J_{lii} is given as

$$J_{lii}\Big|_{i=1,2}=\begin{bmatrix} J_{l11} & J_{l12} \\ J_{l21} & J_{l22} \end{bmatrix} \tag{1}$$

where

$$\begin{aligned} J_{l11} &= M_{L1}(\frac{L_1}{2})^2 + M_2 L_1{}^2 + M_{L2}\left(L_1 + \frac{L_2\cos\theta_{l2}}{2}\right)^2, \\ &+ M_{load}\left(L_1 + L_2\cos\theta_{l2}\right)^2 \\ J_{l12} = J_{l21} &= M_{L2}\left[\left(\frac{L_2\cos\theta_{l2}}{2}\right)^2 + \frac{L_1 L_2\cos\theta_{l2}}{2}\right], \\ &+ M_{load}\left[\left(L_2\cos\theta_{l2}\right)^2 + L_1 L_2\cos\theta_{l2}\right] \\ J_{l22} &= M_{L2}(\frac{L_2}{2})^2 + M_{load} L_2{}^2 . \end{aligned}$$

Therefore, the coupling model of the TITO system can be given by

$$J_o\ddot{X} + D_0\dot{X} + K_0 X = C_0\tau \tag{2}$$

where

$$X = \begin{bmatrix} \theta_{m1} & \theta_{m2} & \theta_{l1} & \theta_{l2} \end{bmatrix}^T ,$$

$$J_0 = \begin{bmatrix} J_{m1} & 0 & 0 & 0 \\ 0 & J_{m2} & 0 & 0 \\ 0 & 0 & J_{l11} & J_{l12} \\ 0 & 0 & J_{l21} & J_{l22} \end{bmatrix},$$

$$D_0 = \begin{bmatrix} B_{m1}+D_1 & 0 & -D_1 & 0 \\ 0 & B_{m2}+D_2 & 0 & -D_2 \\ -D_1 & 0 & B_{l1}+D_1 & 0 \\ 0 & -D_2 & 0 & B_{l2}+D_2 \end{bmatrix},$$

$$K_0 = \begin{bmatrix} K_1 & 0 & -K_1 & 0 \\ 0 & K_2 & 0 & -K_2 \\ -K_1 & 0 & K_1 & 0 \\ 0 & -K_2 & 0 & K_2 \end{bmatrix},$$

$$C_0 = \begin{bmatrix} 1 & 0 & 0 & 0 \\ 0 & 1 & 0 & 0 \end{bmatrix}^T ,$$

$$\tau = \begin{bmatrix} \tau_{m1} & \tau_{m2} \end{bmatrix}^T .$$

The Coulomb frictions, the Coriolis and centrifugal torque of the two-link manipulator are not considered temporally for simplicity.

3. Controller Design

In this paper, a TITO system is controlled in a decentralized structure. A velocity controller is proposed to suppress vibrations and decoupling torque. The proposed controller includes a controller *C*, a decoupler and a RBSO. The decoupler is designed in a simplified structure based on the dynamic model of the TITO system to decrease the influences of the decoupling torque. The RBSO is designed to damp vibrations, containing a SOB and a Damper, as shown in fig. 2.

The RBSO suppresses vibrations by adding system damping after decoupling the TITO system. Therefore, the first step is to design the decoupler.

3.1. Decoupler design

The decoupler is dynamically designed in a simplified structure [17]. In order to facilitate design, the coupling model needs to be equivalently transformed based on the system transfer function built in figure 1(b). Then, the TITO system with a decoupler can be equivalently transformed, as shown in fig. 3.

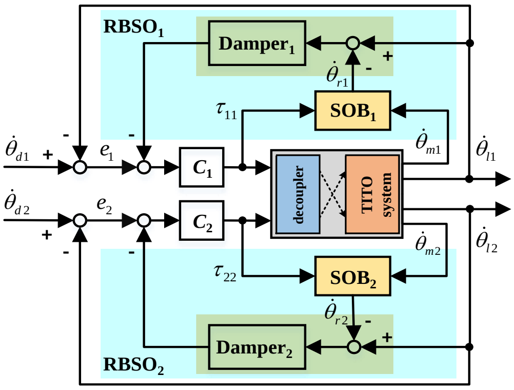

Fig. 2. Block diagram of the proposed method.

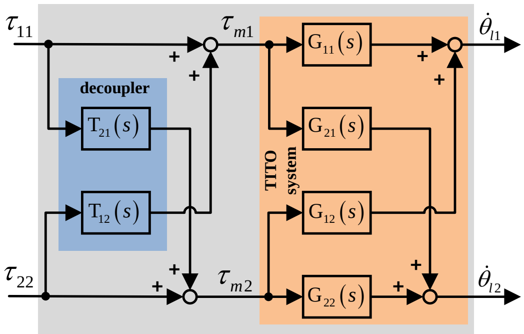

Fig. 3. Block diagram of the TITO system with a decoupler.

In the new TITO system, the transfer functions $G_{11}(s)$, $G_{12}(s)$, $G_{21}(s)$ and $G_{22}(s)$ are given as

$$G_{11}(s)=\frac{D_1 s+K_1}{den_1} \tag{3}$$

$$G_{12}(s)=\sigma_2\cdot\frac{J_{l12}}{J_{l22}}\cdot\frac{num_2}{den_2}\cdot\frac{1}{(J_{l11}s+B_{l1})} \tag{4}$$

$$G_{21}(s)=\sigma_1\cdot\frac{J_{l21}}{J_{l11}}\cdot\frac{num_1}{den_1}\cdot\frac{1}{(J_{l22}s+B_{l2})} \tag{5}$$

$$G_{22}(s)=\frac{D_2 s+K_2}{den_2} \tag{6}$$

where

$$\sigma_1\in[0,1],$$

$$\sigma_2\in[0,1],$$

$$num_1=J_{l11}D_1s^3+(K_1J_{l11}+D_1B_{l1})s^2+(K_1B_{l1})s\,,$$

$$\begin{aligned}den_1=&\,J_{m1}J_{l11}s^4+(J_{m1}B_{l1}+J_{l11}B_{m1}+J_{m1}D_1+J_{l11}D_1)s^3\\&+(J_{m1}K_1+J_{l11}K_1+B_{m1}D_1+B_{l1}D_1+B_{m1}B_{l1})s^2+\\&(B_{m1}K_1+B_{l1}K_1)s\end{aligned}\quad,$$

$$num_2=J_{l22}D_2s^3+(K_2J_{l22}+D_2B_{l2})s^2+(K_2B_{l2})s\,,$$

$$\begin{aligned} den_2 = {} & J_{m2}J_{l22}s^4 + \left(J_{m2}B_{l2} + J_{l22}B_{m2} + J_{m2}D_2 + J_{l22}D_2\right)s^3 \\ & + \left(J_{m2}K_2 + J_{l22}K_2 + B_{m2}D_2 + B_{l2}D_2 + B_{m2}B_{l2}\right)s^2 + \\ & \left(B_{m2}K_2 + B_{l2}K_2\right)s \end{aligned}.$$

The transfer matrix from the inputs of the TITO system $\begin{bmatrix}\tau_{m1} & \tau_{m2}\end{bmatrix}^T$ to the outputs $\begin{bmatrix}\dot{\theta}_{l1} & \dot{\theta}_{l2}\end{bmatrix}^T$ can be established as

$$\begin{bmatrix}\dot{\theta}_{l1} \\ \dot{\theta}_{l2}\end{bmatrix} = \begin{bmatrix}G_{11}(s) & G_{12}(s) \\ G_{21}(s) & G_{22}(s)\end{bmatrix} \cdot \begin{bmatrix}\tau_{m1} \\ \tau_{m2}\end{bmatrix} \tag{7}$$

The transfer matrix from $\begin{bmatrix}\tau_{11} & \tau_{22}\end{bmatrix}^T$ to $\begin{bmatrix}\tau_{m1} & \tau_{m2}\end{bmatrix}^T$ can be established as

$$\begin{bmatrix}\tau_{m1} \\ \tau_{m2}\end{bmatrix} = \begin{bmatrix}1 & T_{12}(s) \\ T_{21}(s) & 1\end{bmatrix} \cdot \begin{bmatrix}\tau_{11} \\ \tau_{22}\end{bmatrix} \tag{8}$$

Therefore, the transfer matrix from $\begin{bmatrix}\tau_{11} & \tau_{22}\end{bmatrix}^T$ to the outputs $\begin{bmatrix}\dot{\theta}_{l1} & \dot{\theta}_{l2}\end{bmatrix}^T$ of the TITO system with a decoupler become

$$\begin{aligned} \begin{bmatrix}\dot{\theta}_{l1} \\ \dot{\theta}_{l2}\end{bmatrix} & = \begin{bmatrix}G_{11}(s) & G_{12}(s) \\ G_{21}(s) & G_{22}(s)\end{bmatrix} \cdot \begin{bmatrix}1 & T_{12}(s) \\ T_{21}(s) & 1\end{bmatrix} \cdot \begin{bmatrix}\tau_{11} \\ \tau_{22}\end{bmatrix} \\ & = \begin{bmatrix}G_{11} + G_{12}T_{21} & G_{11}T_{12} + G_{12} \\ G_{21} + G_{22}T_{21} & G_{21}T_{12} + G_{22}\end{bmatrix} \cdot \begin{bmatrix}\tau_{11} \\ \tau_{22}\end{bmatrix} \end{aligned} \tag{9}$$

To achieve the TITO system decoupled, it needs to diagonalize the transfer matrix from $\begin{bmatrix}\tau_{11} & \tau_{22}\end{bmatrix}^T$ to $\begin{bmatrix}\dot{\theta}_{l1} & \dot{\theta}_{l2}\end{bmatrix}^T$. Then the conditions in equation (10) need to be met.

$$\begin{cases} G_{11}(s)T_{12}(s) + G_{12}(s) = 0 \\ G_{21}(s) + G_{22}(s)T_{21}(s) = 0 \end{cases} \tag{10}$$

Therefore, the decoupler is designed as

$$\begin{cases} T_{12}(s) = -\dfrac{G_{12}(s)}{G_{11}(s)} \\ T_{21}(s) = -\dfrac{G_{21}(s)}{G_{22}(s)} \end{cases} \tag{11}$$

3.2. Rigid-body state observer design

Based on the TITO system decoupled, the RBSO is designed to suppress vibrations in a decentralized structure, as shown in Fig. 2. The rigid-body velocity is a state variable to be observed by SOB_i, as shown in figure 4 [18]. The decoupled $joint_i$ is modelled as a two-inertia system. J_i is the sum of the actual motor-side inertia and actual link-side inertia. J_{ni} is the sum of the nominal motor-side inertia and nominal link-side inertia. $J_{ni} = J_{mi} + J_{lii}$.

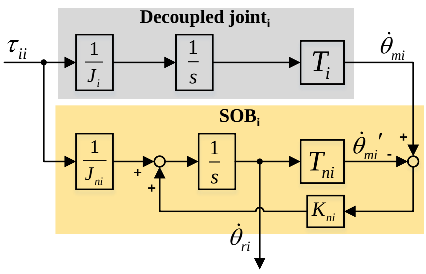

Fig. 4. Block diagram of the SOBi.

In the SOB_i, the transfer function T_{ni} is

$$T_{ni} = \frac{s^2 + \omega_{ai}{}^2}{\omega_{ai}{}^2} \frac{\omega_{ri}{}^2}{s^2 + \omega_{ri}{}^2} \tag{12}$$

where $\omega_{ai} = \sqrt{K_i / J_{lii}}$, $\omega_{ri} = \omega_{ai}\sqrt{1 + J_{lii}/J_{mi}}$.

When the parameter K_{ni} increases, the bandwidth of the SOB$_i$ improves. The rigid-body velocity $\dot{\theta}_{ri}$ can be obtained accurately with the parameter K_{ni} increasing.

Combined with the Damper$_i$ shown in figure 2, the RBSO$_i$ feeds back the error between link velocity $\dot{\theta}_{li}$ and rigid-body velocity $\dot{\theta}_{ri}$ to the controller C_i.

As for the flexible joint$_i$, the open-loop and closed-loop transfer functions from the velocity error e_i to link velocity $\dot{\theta}_{li}$ are given in equations (13) and (14), respectively.

$$P_{openi}(s) = \frac{\dot{\theta}_{li}}{e_i} = \frac{\dot{\theta}_{li}}{\dot{\theta}_{di} - \dot{\theta}_{li}} = \frac{C_i}{J_{ni}s} \cdot \frac{\omega_{ri}{}^2}{s^2 + \omega_{ri}{}^2} \tag{13}$$

$$P_{closei}(s) = \frac{\dot{\theta}_{li}}{e_i} = \frac{\dot{\theta}_{li}}{\dot{\theta}_{di} - \dot{\theta}_{li}} = \frac{C_i}{J_{ni}s} \cdot \frac{\omega_{ri}{}^2}{s^2 - g_i C_i s + \omega_{ri}{}^2} \tag{14}$$

Compared the closed-loop to the open-loop transfer function, the closed-loop transfer function adds a damping term $-g_iC_is$ to the decoupled flexible joint$_i$. When the Damper$_i$ is designed as a negative proportional gain, the system damping of the decoupled flexible joint$_i$ can be increased. Then the vibrations can be damped by the increased system damping [16].

4. Simulations

In order to verify the ability to decrease coupling torque and vibrations, a two-link manipulator model is established in the Simulink of MATLAB, as shown in fig. 5. In the simulation model, the gravity and nonlinear frictions are not considered temporarily.

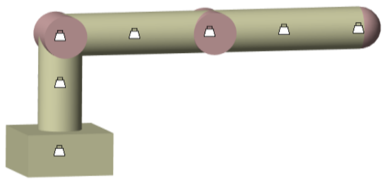

Fig. 5. Simulation model of the two-link manipulator.

The dynamic parameters of the two-link manipulator and the flexible joint$_i$ are set in Table I.

TABLE I. DYNAMIC PARAMETERS OF THE TITO SYSTEM

Notation	Name	Value	Unit
Two-link manipulator			
M_1	Mass of the first flexible joint	2.68	kg
M_2	Mass of the second flexible joint	1.87	kg
L_1	Length of the first link	0.35	m
L_2	Length of the second link	0.35	m
M_{L1}	Mass of the first link	3.54	kg
M_{L2}	Mass of the second link	6.96	kg
M_{load}	Mass of the payload	0	kg
Flexible joint$_i$			
J_{mi}	Motor-side inertia	7.34	kg·m^2
B_{mi}	Motor-side viscous damping	33.28	N·m·s/rad
J_{li}	Link-side inertia	2.26	kg·m^2
B_{li}	Link-side viscous damping	5.00	N·m·s/rad

K_i	Joint stiffness	32500.00	N·m/rad
D_i	Joint damping	10.00	N·m·s/rad
n_i	Reduction ratio of harmonic drive	160	-

There are three comparison strategies to verify the effectiveness of the proposed method:

1. Based on a pure PI controller, compare the simulation results before and after using the decoupler to verify the ability to restrain the coupling torque.

2. Compare the simulation results before and after using the RBSO to verify the effectiveness in suppressing vibrations.

3. Compare the simulation results before and after using the proposed method (Decouple + RBSO) to verify the effectiveness in decreasing coupling torque and vibrations simultaneously.

In simulations, controller C_i is designed as a proportional-integral controller, as KP_i and KI_i. The control parameters of the proposed method are scheduled in Table II.

TABLE II. CONTROL PARAMETERS

Notation	Name	Value
KP_i	proportional gain of C_i	100
KI_i	integral gain of C_i	1000
σ_1	deviation factors of the decoupler	0.6
σ_2		
K_{ni}	gain of SOB_i	600
g_i	proportional gain of $Damper_i$	-0.5

The desired velocity of the first flexible joint is a step waveform. It is actuated at 0.1s, then keeping 300 rpm (0.196 rad/s) for 1.4 s. The desired velocity of the second flexible joint is 0, which will be only actuated by the coupling torque. The simulation results of the three comparison strategies are shown in fig. 6.

The black thin dash line is the desired velocity. The blue thick dash line is the pure PI method. The green thick dotted line is the Decouple method. The red thick dash-dot line is the RBSO method. The black thick solid line is the proposed method (Decouple + RBSO).

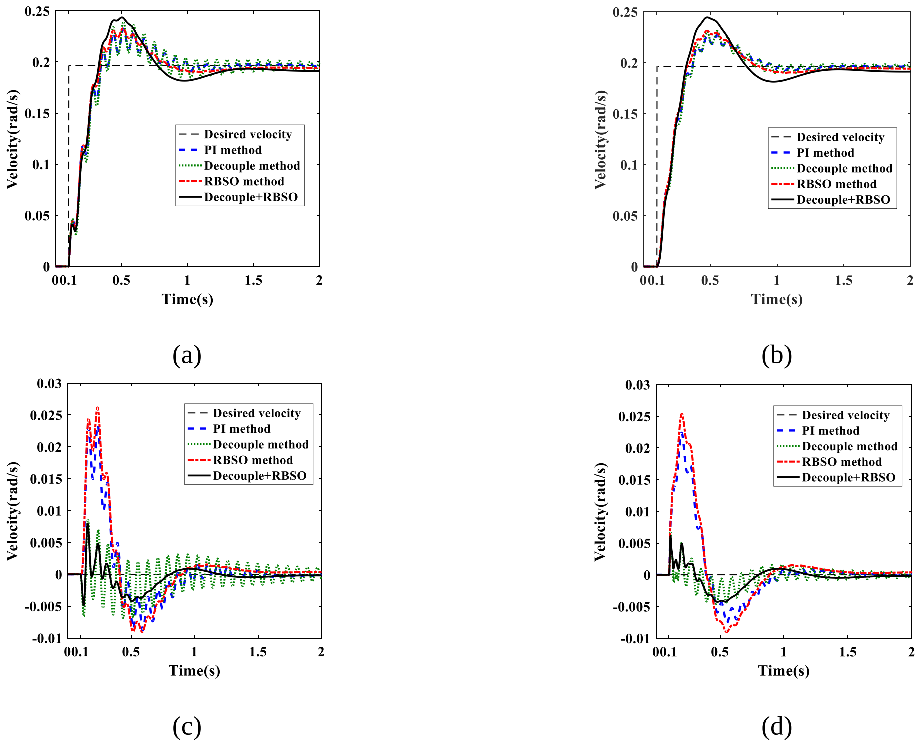

Fig. 6. Simulation results of the two-link manipulator.
(a) Motor velocity tracking of the first flexible joint. (b) Link velocity tracking of the first flexible joint. (c)

Motor velocity tracking of the second flexible joint. (d) Link velocity tracking of the second flexible joint.

The simulation results show that the RBSO method can suppress vibrations effectively, compared with the pure PI method and Decouple method. The Decouple method can decrease coupling torque effectively, compared with the pure PI method and RBSO method. The proposed method (Decouple + RBSO) can damp vibrations and coupling torque simultaneously, compared with the other three methods. Since the deviation factors, σ_1 and σ_2 are set less than 1, which means the coupling torque can only be partially decoupled but not completely decoupled, as shown in fig. 6(c) and fig. 6(d).

5. Conclusion

A velocity controller for a TITO system in a decentralized structure to damp coupling torque and vibrations is proposed in this paper. The proposed controller decouples the coupling torque using a dynamic decoupler in a simplified structure. Based on the decoupled joint system, the proposed controller suppresses vibrations using a rigid-body state observer (RBSO) combined with a proportional-integral controller by adding system damping. Some comparisons among a pure PI method, a Decouple method, a RBSO method and the proposed method (Decouple + RBSO) are discussed, which verify the ability to damp coupling torque and vibrations of the proposed method.

6. Acknowledgment

This work was supported by the National Key R&D Program of China (2019YFB1309900), the National Natural Science Foundation of China (51805523, U1813223, U20A20282, 92048201), the International Partnership Program of the Chinese Academy of Sciences (174433KYSB20190036), the Key R&D Program of Zhejiang Province (2019C01043 and 2021C01067), the Ningbo Science and Technology Innovation 2025 Major Special Project (2021Z128).

7. References

[1] L. Lan, "A Study on High Performance Control for Industrial Robot Manipulators," Kyushu Institute of Technology, 2014.

[2] Q. Xin *et al.*, "A Robust Method Based on Dual Encoders to Eliminate Velocity Ripple for Modular Drive Joints," *Actuators,* vol. 9(4), p. 135, 2020.

[3] J. Kim and E. A. Croft, "Preshaping input trajectories of industrial robots for vibration suppression," *Robotics and Computer Integrated Manufacturing,* vol. 54, no. DEC., pp. 35-44, 2018.

[4] T. V. Trung and M. Iwasaki, "Robust 2-DoF Controller Design using H∞ Synthesis for Flexible Robots," *IEEJ Journal of Industry Applications,* vol. 8, no. 4, pp. 623-631, 2019.

[5] M. Nazemizadeh, M. Taheri, and S. Nazeri, "The application of fuzzy-logic method to control of robots: a review study," *International Journal of Mechanical Engineering and Robotics Research,* vol. 3, no. 2, p. 229, 2014.

[6] S. Zhang, Y.-h. Zhang, X.-n. Zhang, and G.-x. Dong, "Fuzzy PID control of a two-link flexible manipulator," *Journal of Vibroengineering,* vol. 18, no. 1, pp. 250-266, 2016.

[7] Y. Marushita, H. Ikeda, and H. Sugie, "Vibration suppression control using the load-side acceleration feedback," in *IECON 2007-33rd Annual Conference of the IEEE Industrial Electronics Society*, 2007, pp. 810-815: IEEE.

[8] Q. Xin, C. Wang, C.-Y. Chen, G. Yang, Z. Fang, and H. Chen, "Vibration Suppression Method Based on the Equivalent Rigid Body State Observer of Modular Joint for a Collaborative Robot," in *Advances in Manufacturing Technology XXXIII*: IOS Press, 2019, pp. 147-152.

[9] D. P. Nam, P. T. Loc, N. Huong, and D. T. Tan, "A finite-time sliding mode controller design for flexible joint manipulator systems based on disturbance observer," *International Journal of Mechanical Engineering and Robotics Research,* vol. 8, no. 4, pp. 619-625, 2019.

[10] J. N. Yun and J.-B. Su, "Design of a disturbance observer for a two-link manipulator with flexible joints," *IEEE Transactions on Control Systems Technology,* vol. 22, no. 2, pp. 809-815, 2013.

[11] L. Liu, S. Tian, D. Xue, T. Zhang, Y. Q. Chen, and S. Zhang, "A Review of Industrial MIMO Decoupling Control," *International Journal of Control, Automation and Systems,* 2019.

[12] J. Lee, D. Hyun Kim, and T. F. Edgar, "Static decouplers for control of multivariable processes," *AIChE journal*, vol. 51, no. 10, pp. 2712-2720, 2005.

[13] T. V. Trung and M. Iwasaki, "High-Performance Positioning using Decoupling Controllers for Flexible Two-Link Robots with Strain Wave Gears," *IEEJ Journal of Industry Applications*, vol. 9, no. 4, pp. 408-417, 2020.

[14] X. Gao and Y. Weng, "Adaptive Sliding Mode Decoupling Control with Data-Driven Sliding Surface for Unknown MIMO Nonlinear Discrete Systems," *Circuits, systems, and signal processing: CSSP*, 2017.

[15] C. Wang, W. Zhao, Z. Luan, Q. Gao, and K. Deng, "Decoupling control of vehicle chassis system based on neural network inverse system," Mechanical *Systems & Signal Processing*, 2018.

[16] Q. Xin, C. Wang, C.-Y. Chen, G. Yang, and L. Chen, "Robust Vibration Control Based on Rigid-Body State Observer for Modular Joints," *Machines*, vol. 9, no. 9, p. 194, 2021.

[17] T. V. Trung and M. Iwasaki, "A Decoupling 2-DoF Control Design for Lightweight Two-Link Robots," in *IECON 2019 - 45th Annual Conference of the IEEE Industrial Electronics Society*, 2019.

[18] Q. Xin, C. Wang, C.-Y. Chen, and G. Yang, "A Vibration Suppression Controller Design for a Two-Link Manipulator with Flexible Joints," in 2021 3rd International Symposium on Robotics & Intelligent Manufacturing Technology (ISRIMT), 2021, pp. 454-458: IEEE